Supplement of Atmos. Chem. Phys., 18, 9845–9860, 2018
https://doi.org/10.5194/acp-18-9845-2018-supplement

Atmospheric Chemistry and Physics
Open Access
EGU

Supplement of

Morphological transformation of soot: investigation of microphysical processes during the condensation of sulfuric acid and limonene ozonolysis product vapors

Xiangyu Pei et al.

Correspondence to: Ravi Kant Pathak (ravikant@chem.gu.se)

Reproducibility of soot

For high quality data, reproducibility of the flame in all experiments was ensured. The mass and number concentrations were measured four times during the entire measurement to guarantee that the same soot particles were generated. Figure S1 and Figure S2 show the particle mass and number concentration, respectively, associated with four sizes of fresh soot.

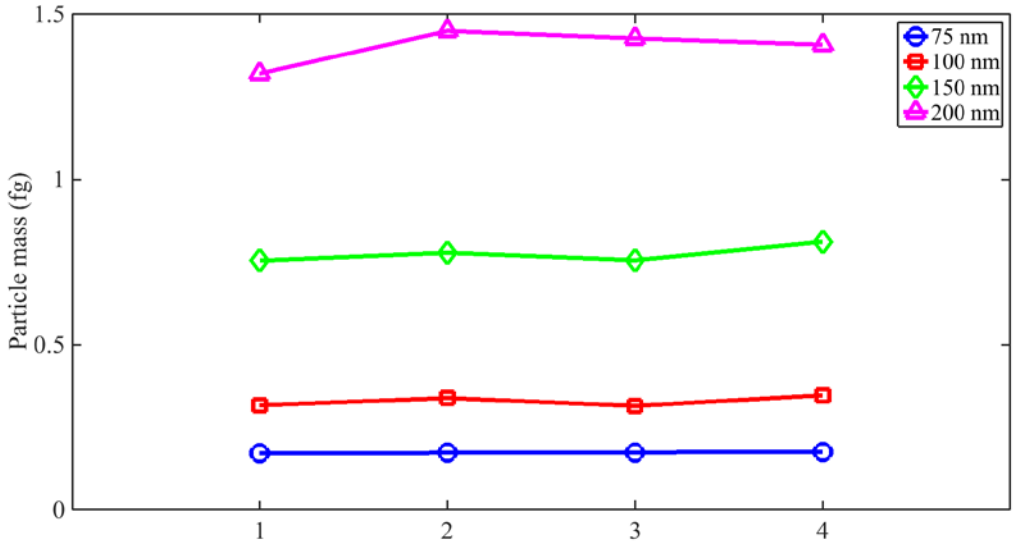

Figure S1. Particle mass of fresh soot with mobility size of 75, 100, 150, and 200 nm during the measurement.

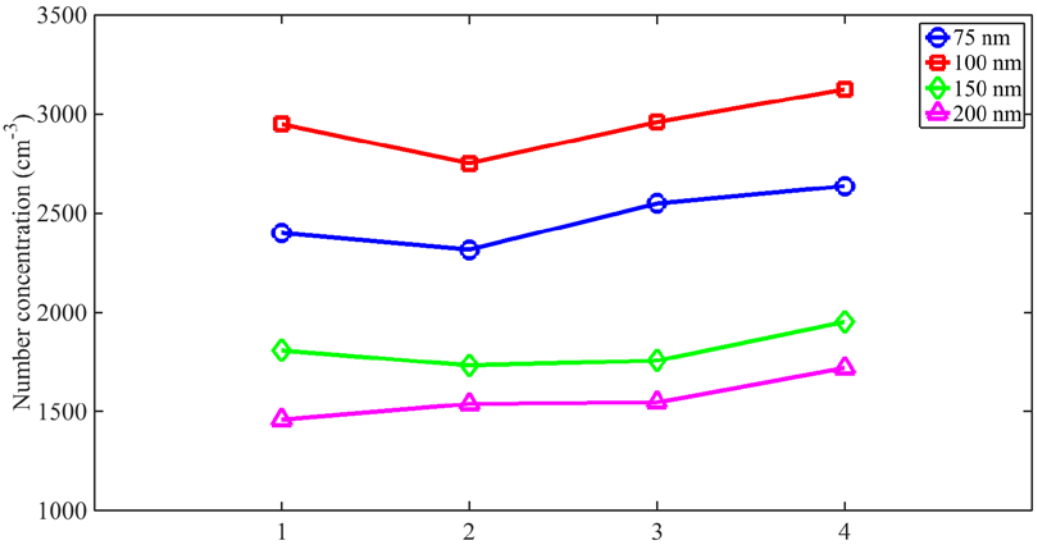

Figure S2. Number concentration of fresh soot with mobility size of 75, 100, 150, and 200 nm during the measurement.

Correction of multiply charged particles

The DMA-APM-CPC scans were fitted by normal distributions. The DMA-APM-CPC system can distinguish between singly and multiply charged (mainly doubly) spherical particles. However, for soot aggregates with effective densities that decrease with increasing mobility diameter, this distinction is possible in only some cases. The doubly charged particles may result in the overestimation of the particle mass and the effective density. The fraction of doubly charged particles may influence the mobility diameter of the soot aggregates if this diameter is smaller than the geometric mean diameter (GMD; in this study: 90 nm) of the particle number size distribution. Therefore, a sensitivity test was conducted for the 75-nm soot, assuming a Boltzmann charge distribution. The overestimation of the mass of the 75-nm soot was <5%, whereas the overestimation of the masses of the 100-nm, 150-nm, and 200-nm soot was negligible, which is consistent with the literature (Rissler et al., 2013).

Experimental conditions

Table S1 shows the experiments performed and results obtained under different coating conditions.

Table S1. Experiments performed and results obtained under different coating conditions.

Exp.	Mobility diameter of fresh soot (nm)	Sulfuric acid bath T (°C)	VOC bath T (°C)	Soot core mass (fg)	Sulfuric acid mass (fg)	SOA mass (fg)	Limonene concentration ($\mu g \cdot m^{-3}$)	Coating thickness, Δr_{me} (nm)	Diameter growth factor, *Gfd*	Effective density, ρ_{eff} ($g \cdot cm^{-3}$)	Dynamic shape factor, χ	Void space fraction, F_{vs}
1	75	bypass	UV off	0.17	0.00	0.00	0	0	1.00	0.80	1.62	0.58
2	75	bypass	1	0.17	0.00	0.08	56	5.7	1.11	0.88	1.39	0.45
3	75	bypass	5	0.17	0.00	0.11	73	7.4	1.12	0.99	1.27	0.37
4	75	1	UV off	0.17	0.02	0.00	0	1.3	1.00	0.86	1.55	0.52
5	75	1	1	0.17	0.02	0.13	56	8.9	1.14	1.02	1.26	0.35
6	75	1	5	0.17	0.02	0.12	73	8.5	1.16	0.96	1.31	0.40
7	75	1	15	0.17	0.02	0.63	138	24.8	1.58	0.96	1.19	0.29
8	75	5	UV off	0.17	0.03	0.00	0	1.4	0.98	0.86	1.55	0.53
9	75	5	1	0.17	0.03	0.15	56	9.8	1.13	0.98	1.27	0.33
10	75	5	5	0.17	0.03	0.26	73	14.3	1.22	1.03	1.20	0.26
11	75	5	15	0.17	0.03	0.91	138	30.6	1.59	1.05	1.11	0.13

12	75	25	UV off	0.17	0.26	0.00	0	9.9	1.19	1.20	1.27	0.37
13	75	25	1	0.17	0.26	0.61	56	27.6	1.64	1.09	1.15	0.25
14	75	25	5	0.17	0.26	0.70	73	29.4	1.71	1.08	1.15	0.27
15	75	25	15	0.17	0.26	2.37	138	52.1	2.11	1.11	1.07	0.05
16	100	bypass	UV off	0.33	0.00	0.00	0	0	1.00	0.64	1.83	0.63
17	100	bypass	1	0.33	0.00	0.15	56	4.9	1.07	0.85	1.55	0.56
18	100	bypass	5	0.33	0.00	0.18	73	6.4	1.10	0.82	1.54	0.54
19	100	bypass	15	0.33	0.00	0.35	138	12.1	1.18	0.90	1.37	0.45
20	100	1	UV off	0.33	0.01	0.00	0	0.1	1.01	0.69	1.74	0.63
21	100	1	1	0.33	0.01	0.19	56	8.2	1.10	0.86	1.39	0.47
22	100	1	5	0.33	0.01	0.20	73	8.5	1.13	0.81	1.44	0.50
23	100	1	15	0.33	0.01	0.39	138	14.2	1.19	0.97	1.24	0.39
24	100	5	UV off	0.33	0.04	0.00	0	2.0	1.01	0.67	1.78	0.60
25	100	5	1	0.33	0.04	0.20	56	10.0	1.10	0.85	1.40	0.45
26	100	5	5	0.33	0.04	0.24	73	11.1	1.13	0.90	1.35	0.46
27	100	5	15	0.33	0.04	0.52	138	18.7	1.23	0.94	1.25	0.32
28	100	25	UV off	0.33	0.34	0.00	0	8.8	1.07	1.08	1.35	0.43
29	100	25	1	0.33	0.34	0.27	56	16.2	1.23	1.12	1.22	0.39
30	100	25	5	0.33	0.34	0.45	73	20.3	1.34	1.07	1.21	0.41
31	100	25	15	0.33	0.34	1.50	138	36.8	1.59	1.07	1.13	0.24
32	150	bypass	UV off	0.75	0.00	0.00	0	0.0	1.00	0.46	2.13	0.73
33	150	bypass	1	0.77	0.00	0.28	56	5.0	1.02	0.63	1.79	0.65
34	150	bypass	5	0.77	0.00	0.29	73	5.9	1.04	0.59	1.84	0.66
35	150	1	UV off	0.77	0.01	0.00	0	0.1	1.01	0.43	2.20	0.74
36	150	1	1	0.77	0.01	0.28	56	7.2	1.04	0.59	1.73	0.63
37	150	1	5	0.77	0.01	0.34	73	8.5	1.06	0.62	1.66	0.62
38	150	1	15	0.77	0.01	0.59	138	13.5	1.09	0.68	1.53	0.56
39	150	5	UV off	0.77	0.12	0.00	0	2.7	1.02	0.50	2.05	0.71
40	150	5	1	0.77	0.12	0.35	56	10.7	1.07	0.61	1.68	0.60
41	150	5	5	0.77	0.12	0.49	73	13.4	1.09	0.68	1.55	0.57
42	150	5	15	0.77	0.12	0.88	138	19.8	1.13	0.78	1.39	0.48
43	150	25	UV off	0.77	0.69	0.00	0	10.4	1.02	0.81	1.55	0.55
44	150	25	1	0.77	0.69	0.74	56	22.1	1.11	0.97	1.28	0.38
45	150	25	5	0.77	0.69	0.94	73	24.7	1.16	0.95	1.28	0.40

46	150	25	15	0.77	0.69	1.90	138	35.2	1.30	1.08	1.15	0.36
47	200	bypass	UV off	1.46	0.00	0.00	0	0	1.00	0.38	2.31	0.78
48	200	bypass	1	1.46	0.00	0.39	56	6.5	0.98	0.53	1.92	0.68
49	200	bypass	5	1.46	0.00	0.43	73	7.1	0.98	0.54	1.89	0.68
50	200	bypass	15	1.46	0.00	0.92	138	14.4	1.05	0.61	1.67	0.64
51	200	1	UV off	1.46	0.04	0.00	0	0.4	1.01	0.44	2.11	0.75
52	200	1	1	1.46	0.04	0.44	56	7.3	1.01	0.56	1.77	0.66
53	200	1	5	1.46	0.04	0.58	73	9.2	1.01	0.59	1.69	0.63
54	200	1	15	1.46	0.04	0.82	138	12.3	1.05	0.59	1.66	0.63
55	200	5	UV off	1.46	0.10	0.00	0	1.7	1.00	0.40	2.23	0.78
56	200	5	1	1.46	0.10	0.53	56	10.4	1.01	0.48	1.87	0.67
57	200	5	5	1.46	0.10	0.58	73	11.0	1.02	0.50	1.85	0.67
58	200	5	15	1.46	0.10	1.27	138	19.6	1.07	0.59	1.60	0.59
59	200	25	UV off	1.46	0.68	0.00	0	8.5	0.96	0.61	1.78	0.66
60	200	25	1	1.46	0.68	0.34	56	13.2	1.01	0.64	1.67	0.63
61	200	25	5	1.46	0.68	0.80	73	18.8	1.01	0.76	1.47	0.54
62	200	25	15	1.46	0.68	2.00	138	30.5	1.10	0.86	1.30	0.46

Contribution of restructuring and condensational growth to *Gfd*

Table S2. Contribution of restructuring and condensational growth to *Gfd*.

Exp.	Mobility diameter of fresh soot (nm)	Sulfuric acid bath T (°C)	VOC bath T (°C)	Void space fraction, F_{vs}	Coating thickness, Δr_{me} (nm)	Δr_{me} for filling (nm)	Δr_{me} for growth (nm)	Void space filled (%)	% of material consumed during filling	% of material consumed during growth
1	75	bypass	UV off	0.58	0.0	0	0	0	0	0
2	75	bypass	1	0.45	5.7	1.5	4.2	12	23	77
3	75	bypass	5	0.37	7.4	3.0	4.4	26	35	65
4	75	1	UV off	0.52	1.3	1.3	0.1	10	93	7
5	75	1	1	0.35	8.9	3.6	5.3	31	34	66
6	75	1	5	0.40	8.5	2.5	6.0	21	24	76
7	75	1	15	0.29	24.8	3.3	21.5	28	7	93
8	75	5	UV off	0.52	1.4	1.4	0	10	100	0
9	75	5	1	0.33	9.8	5.0	4.8	46	44	56
10	75	5	5	0.26	14.3	6.2	8.1	59	34	66
11	75	5	15	0.13	30.6	8.4	22.2	86	15	85

12	75	25	UV off	0.37	9.9	2.9	7.0	25	23	77
13	75	25	1	0.25	27.6	3.7	23.9	32	7	93
14	75	25	5	0.27	29.4	2.8	26.6	24	4	96
15	75	25	15	0.05	52.1	9.3	42.8	97	6	94
16	100	bypass	UV off	0.63	0.0	0	0	0	0	0
17	100	bypass	1	0.56	4.9	1.2	3.7	6	22	78
18	100	bypass	5	0.54	6.4	1.7	4.7	9	23	77
19	100	bypass	15	0.45	12.1	3.1	9.0	17	20	80
20	100	1	UV off	0.63	0.1	0.1	0	0	100	0
21	100	1	1	0.47	8.2	3.1	5.1	17	33	67
22	100	1	5	0.50	8.5	2.0	6.5	10	20	80
23	100	1	15	0.39	14.2	4.6	9.6	26	25	75
24	100	5	UV off	0.60	2.0	1.7	0.3	9	84	16
25	100	5	1	0.45	10.0	4.9	5.1	28	43	57
26	100	5	5	0.46	11.1	4.4	6.7	24	33	67
27	100	5	15	0.32	18.7	7.3	11.4	44	29	71
28	100	25	UV off	0.43	8.8	5.2	3.6	30	54	46
29	100	25	1	0.39	16.2	4.6	11.6	26	21	79
30	100	25	5	0.41	20.3	3.4	16.9	18	11	89
31	100	25	15	0.24	36.8	7.3	29.5	44	10	90
32	150	bypass	UV off	0.73	0.0	0	0	0	0	0
33	150	bypass	1	0.65	5.0	3.6	1.4	9	70	30
34	150	bypass	5	0.66	5.9	3.0	2.9	8	48	52
35	150	1	UV off	0.74	0.1	0.1	0	0	100	0
36	150	1	1	0.63	7.2	4.2	3.0	11	55	45
37	150	1	5	0.62	8.5	4.3	4.2	11	47	53
38	150	1	15	0.56	13.5	6.4	7.1	18	41	59
39	150	5	UV off	0.71	2.7	1.1	1.6	3	39	61
40	150	5	1	0.60	10.7	5.8	4.9	16	49	51
41	150	5	5	0.57	13.4	6.9	6.5	19	45	55
42	150	5	15	0.48	19.8	9.8	10.0	29	41	59
43	150	25	UV off	0.55	10.4	8.7	1.7	25	81	19
44	150	25	1	0.38	22.1	14.0	8.1	45	55	45
45	150	25	5	0.40	24.7	12.6	12.1	39	41	59
46	150	25	15	0.36	35.2	12.4	22.8	39	24	76
47	200	bypass	UV off	0.78	0.0	0	0	0	0	0
48	200	bypass	1	0.68	6.5	6.5	0	10	100	0
49	200	bypass	5	0.68	7.1	7.1	0	12	100	0
50	200	bypass	15	0.64	14.4	9.2	5.2	15	59	41
51	200	1	UV off	0.75	0.4	0.4	0	1	100	0
52	200	1	1	0.66	7.3	7.3	0	12	100	0
53	200	1	5	0.63	9.2	8.4	0.8	14	90	10
54	200	1	15	0.63	12.3	8.2	4.1	14	62	38

55	200	5	UV off	0.78	1.7	1.4	0.3	2	82	18
56	200	5	1	0.67	10.4	9.7	0.7	16	92	8
57	200	5	5	0.67	11.0	9.4	1.6	16	83	17
58	200	5	15	0.59	19.6	12.8	6.8	23	59	41
59	200	25	UV off	0.66	8.5	8.5	0	14	100	0
60	200	25	1	0.63	13.2	13.2	0	24	100	0
61	200	25	5	0.54	18.8	18.1	0.7	35	95	5
62	200	25	15	0.46	30.5	20.5	10.0	41	58	42

Particle growth in mass

The particle mass was determined via DMA-APM. The particle mass growth factor, *Gfm*, is determined from:

$$Gfm = \frac{m_p}{m_0} \tag{2}$$

where m_0 and m_p represent the masses of particles before and after coating, respectively.

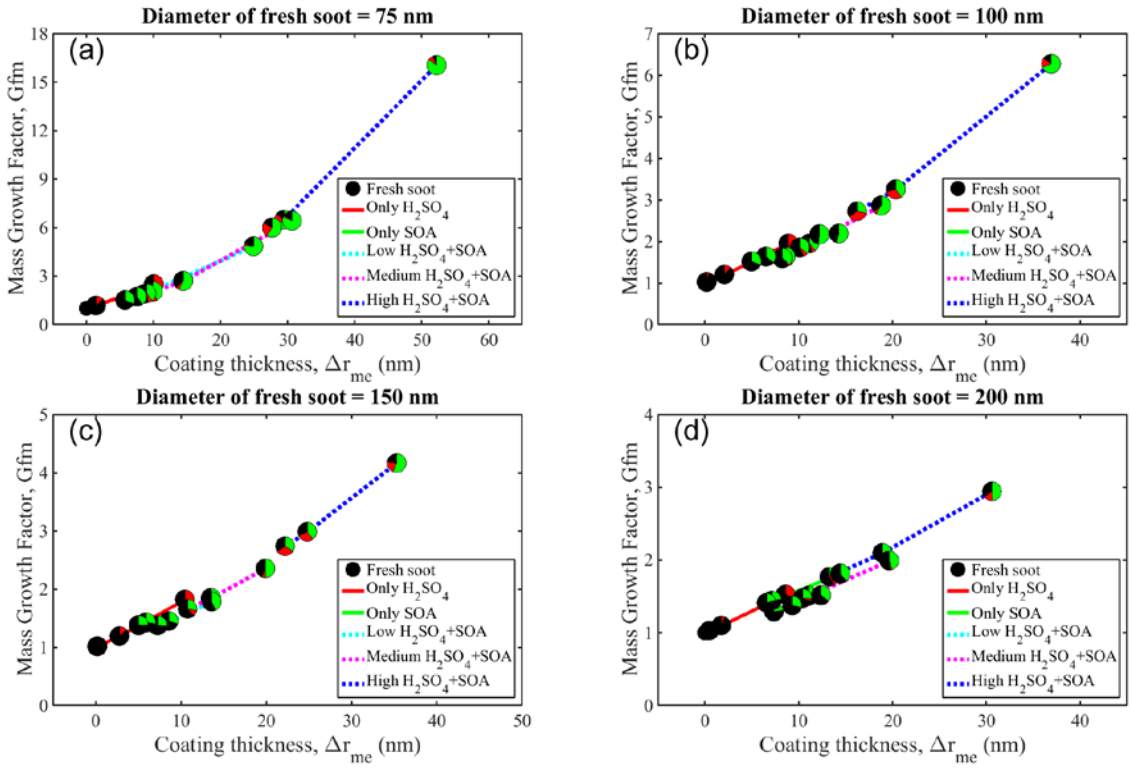

Figure S3. Mass growth factor associated with different mobility sizes (75, 100, 150, and 200 nm) of initial fresh soot.

Figure S3 shows the growth of the particle mass (*Gfm*) for four sizes of fresh soot subjected to different coating conditions as a function of the mass equivalent coating thickness (Δr_{me}). *Gfm* increases significantly when the initial fresh soot size is small compared with the maximum size. *Gfm* increases to 16.00, 6.26, 4.15, and 2.94 for initial fresh-soot sizes of 75 nm, 100 nm, 150 nm, and 200 nm, respectively. This indicates that the core size of the initial soot can determine the evolution of *Gfm*.

Figure S4 and Table S3 show the fitted curves of *Gfm* for soot core sizes.

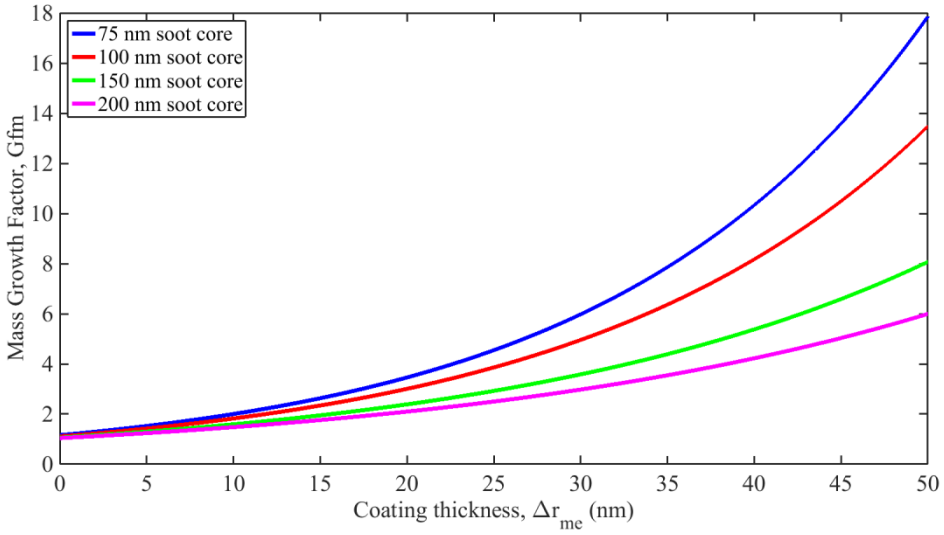

Figure S4. Fitted curves of *Gfm* as a function of Δr_{me} for four soot core sizes.

Using Eq. (3), *Gfm* was fitted as a function of Δr_{me}.

$$Gfm = a \cdot \exp(b \cdot \Delta r_{me}) \quad (3)$$

Ideal growth curve of effective density

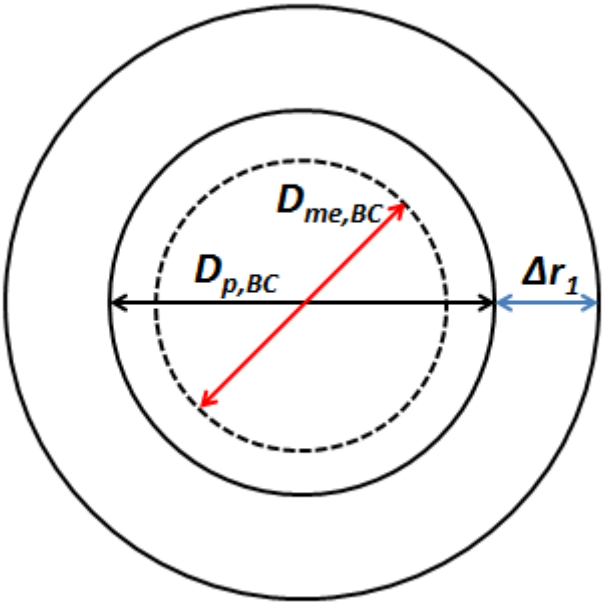

Figure S5. Schematic of calculating ideal growth curve of effective density.

The method of calculating the ideal growth curve of effective density is as follows:

$$m_p = \frac{\pi}{6}\left\{\rho_{eff,BC} \cdot {D_{p,BC}}^3 + \rho_{m,c}\left[\left(D_{p,BC} + 2\Delta r_1\right)^3 - {D_{p,BC}}^3\right]\right\} \quad (4)$$

$$\bar{\rho}_m = \frac{m_p}{\frac{\pi}{6}\frac{\rho_{eff,BC}}{\rho_{m,BC}} \cdot {D_{p,BC}}^3 + \frac{\pi}{6}\left[\left(D_{p,BC} + 2\Delta r_1\right)^3 - {D_{p,BC}}^3\right]} \quad (5)$$

$$\Delta r_2 = \frac{1}{2}\left(\sqrt[3]{\frac{6m_p}{\pi\bar{\rho}_m}} - \sqrt[3]{\frac{\rho_{eff,BC} \cdot {D_{p,BC}}^3}{\rho_{m,BC}}}\right) \quad (6)$$

$$\rho_{eff} = \frac{6m_p}{\pi\left(D_{p,BC} + 2\Delta r_2\right)^3} \quad (7)$$

where $\rho_{eff,BC}$ and $D_{p,BC}$ are effective density and mobility diameter of BC core, respectively. $\rho_{m,BC}$ and $\rho_{m,c}$ are material densities of pure BC (1.77 g cm^{-3}) and coating material (organic: 1.20 g cm^{-3}, sulfuric acid: 1.84 g cm^{-3}), respectively. m_p, $\bar{\rho}_m$and ρ_{eff} are mass, average material density and effective density of coated particle, respectively. Δr_1 and Δr_2 are coating thickness based on mobility diameter and mass equivalent coating thickness, respectively (shown in Figure S5). The ideal growth curve is plotted as ρ_{eff} against Δr_2.

Table S4. Morphology of fresh soot coated with various compounds, as illustrated in Fig. 5.

Literature	Coating compound(s)	$D_{p,0}$ (nm)	$D_{me,0}$ (nm)	*Dfm*	d_{pp} (nm)
Pagels et al. (2009)	Sulfuric acid	75	30.2	2.15	15
Xue et al. (2009)	Glutaric acid (GA), succinic acid (SA)	80	32.9	2.20	16
Qiu et al. (2012)	Toluene-OH oxidation products	100	61.9	2.17	21
Khalizov et al. (2013)	Isoprene-OH oxidation products	100	61.9	2.20	19
Peng et al. (2016)	SOA from ambient precursors	100	63.4	2.25	16
Guo et al. (2016)	m-Xylene-OH oxidation products	100	61.4	2.17	45
Ghazi and Olfert (2013)	Dioctyl sebacate	100	51.9	2.14	45
This study	Sulfuric acid, acidity-mediated limonene SOA	100	70.8	2.28	28

Table S5. Data of mass associated with different levels of sulfuric acid and limonene SOA coatings for the 200 nm soot core, as illustrated in Fig. 3.

	Pure SOA (fg)	Low H_2SO_4 (fg)	Medium H_2SO_4 (fg)	High H_2SO_4 (fg)
H_2SO_4	0	0.04	0.10	0.68

Low SOA	0.39	0.44	0.53	0.34
Medium SOA	0.43	0.58	0.58	0.80
High SOA	0.92	0.82	1.27	2.00

References

Rissler, J., Messing, M. E., Malik, A. I., Nilsson, P. T., Nordin, E. Z., Bohgard, M., Sanati, M., and Pagels, J. H.: Effective Density Characterization of Soot Agglomerates from Various Sources and Comparison to Aggregation Theory, Aerosol Sci.Technol., 47, 792–805, 10.1080/02786826.2013.791381, 2013.